

# Impacts of sagebrush vegetation in a desert climate on the atmospheric boundary layer

Byron Eng, Matthew Moody, and Travis Morrison

May 1, 2017

## 1 Introduction

The Mountain Terrain Atmospheric Modeling and Observations (MATERHORN, ?) Program provides an array of atmospheric observations suitable to investigate and advance many areas of scientific interest. Near-surface flow in areas with vegetation and complex terrain remains an area of weakness in current Numerical Weather Prediction (NWP) models, turbulence closure models, and boundary layer parameterizations (?). In this study, boundary layer characteristics from two MATERHORN observation sites (Sagebrush and Playa) are investigated. The contrast in surface roughness between the two sites are expected to affect dissipation, mixing, and heat flux.

## 2 Results

Data was provided from the Sagebrush and Playa sites for October 18-19th. Both sites harvested data from meteorological towers equipped with fast response sonic anemometers (C-SAT), and finewire thermocouples at multiple heights (18.8 m, 10.15 m, 5.87 m, 2.04 m, and 0.55 m for Sagebrush and 25.5 m, 19.4 m, 10.4 m, 5.3 m, 2.02 m, 0.61m for Playa). The variables measured were the three components of velocity (captured at 20 Hz), temperature, relative humidity (captured at 1 Hz). As a post-processing step the velocity data components were rotated to a Cartesian coordinate system based on 30-minute block averages, with  $u$  denoting the mean wind direction,  $v$  as the velocity horizontally perpendicular to the mean flow, and  $w$  as the vertical velocity. Fluctuations from the mean were also calculated from a 30-minute block average.

$\bar{u}$ ,  $\bar{v}$ , and  $\bar{w}$  were calculated using the rotated velocity data.  $\bar{v}$  and  $\bar{w}$  are close to zero (order of  $10^{-4}$  and  $10^{-5}$ , respectively) for the entire observation period (Figures 1 and 2) verifying that the rotation algorithm performed as expected. Velocity perturbations ( $u'$ ,  $v'$ , and  $w'$ ) were calculated using these mean values. Temperature perturbations ( $T'$ ) and 30-minute block averages ( $\bar{T}$ ) were also calculated.

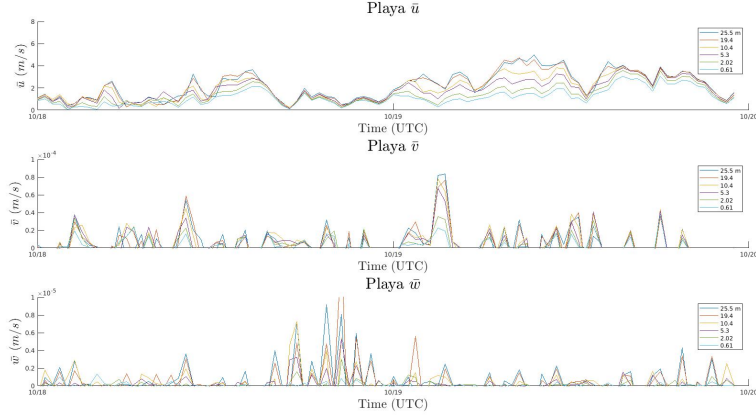


Figure 1: 30-minute block averages of  $\bar{u}$ ,  $\bar{v}$ , and  $\bar{w}$  from the Playa.

Sensible heat flux ( $H_s$ ) was calculated for both sites using Equation 1. Where  $C_p$  is the specific heat of dry air at constant pressure, and  $\rho$  is the density of air.

$$H_s = C_p \cdot \rho \cdot \overline{w'T'} \quad (1)$$

Turbulence kinetic energy ( $TKE$ ) was calculated for both sites using Equation 2.

$$TKE = \frac{1}{2} \overline{u'^2 + v'^2 + w'^2} \quad (2)$$

Figure 3 shows comparisons for  $H_s$  and  $TKE$  at both sites. Vegetation at the Sagebrush site appears to inhibit sensible heat flux at heights below 2 m, indicating surface heat storage induced by vegetation. Sagebrush near-surface  $TKE$  also appears inhibited by vegetation which is compensated by a sharp  $TKE$  increase just above the surface. The Playa site shows a more uniform distribution of  $TKE$  and  $H_s$  at all observed heights.

$$L = \frac{u_*}{\kappa \overline{w'T'}} \quad (3)$$

Equation 3 shows the calculation used for Obukhov length ( $L$ ), where  $\kappa$  is the Kolmogorov constant (assumed equal to 0.4), and  $u_* = \sqrt[4]{\overline{u'w'^2} + \overline{v'w'^2}}$ . The time series of  $L$  (Figure 4) show that the Playa had more near-surface instability during the observation period. However, approximately 2 meters above the surface  $L$  at the Playa remained near zero for the majority of the observation period while  $L$  fluctuated between positive and negative with greater amplitude at the Sagebrush site.

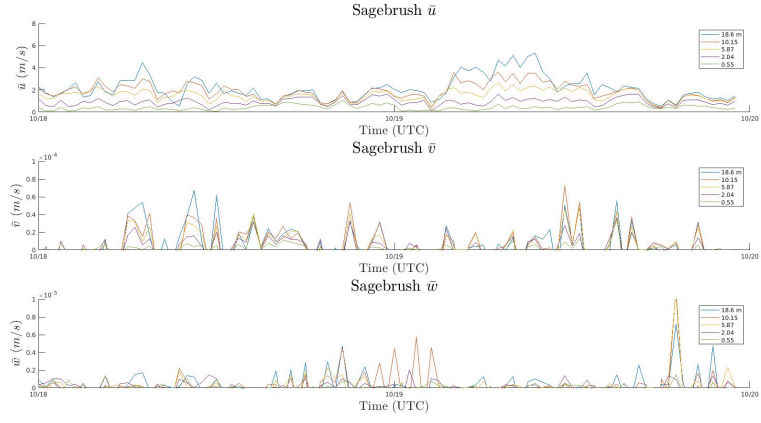


Figure 2: 30-minute block averages of  $\bar{u}$ ,  $\bar{v}$ , and  $\bar{w}$  from the Sagebrush site.

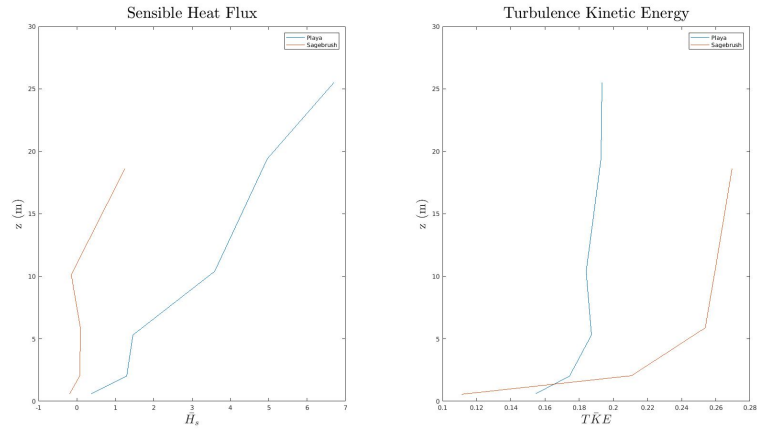


Figure 3:  $H_s$  and  $TKE$  comparisons. Values at each height were averaged over the observation period.

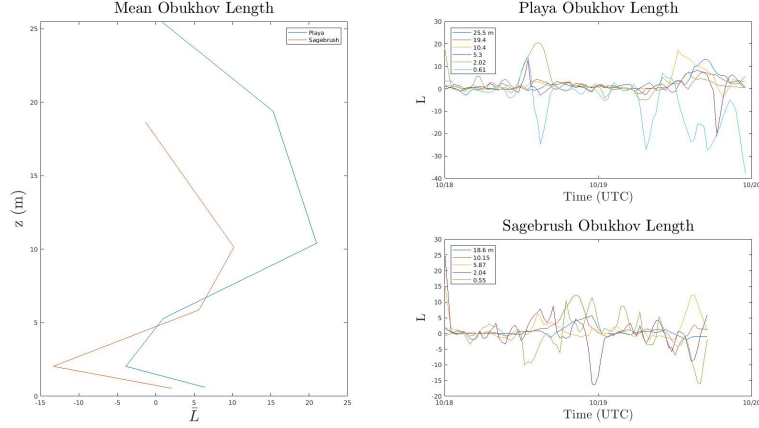


Figure 4: Obukhov length comparison. Mean Obukhov length plotted at each height (**left**), and time series (**right**) for both sites. Time series data were smoothed, giving little weight to outliers, using a variation of Loess Smoothing.

To better understand the impacts of vegetation on boundary layer flow, examination of a highly convective time, 1500-1530 MST (2100-2130 UCT), was further analyzed.

The Probability Distribution Function (PDF) for this time period was calculated for each velocity component and temperature at all heights (Figure 5). The largest contrast between the two sites exists in the PDF between the mean wind velocity component ( $u$ ) and the temperature. Beginning with  $u$  at the sagebrush site the velocity distribution's mean value shifts towards larger values with height, while at the Playa a more uniform mean velocity is maintained across all heights. Additionally, insightful differences between the temperature PDF's between the two sites is observed. At the Sagebrush site, the 0.55 m and 2.04 m sonics report much larger mean temperature values ( $\sim 19.5^\circ \text{C}$ ) than the other heights ( $\sim 16.5^\circ \text{C}$ ), while at the Playa site, the temperature remains uniform with height ( $\sim 15\text{-}16.5^\circ \text{C}$ ). Note at the Sagebrush site the temperature PDF at 0.55 m shows the largest variance. A potential explanation of this observation is that at the low near surface velocities due to the vegetation at Sagebrush decrease convection, hence increasing energy storage within this near surface layer, resulting in higher near-surface temperatures. Table 2 and Table 2 present the kurtosis and skewness with height of velocity and temperature. The red and blue color boxes correlate to the near surface  $u$  velocity at both sites. At the Sagebrush the skewness nears 0 at the surface, increasing with height. While the kurtosis remains less than 3. At the Playa, there is a positive skew near the surface on the mean wind direction, which decreases with height. A decreasing kurtosis in the same signal at the Playa is also observed.

Figure 6 presents the Cumulative Distribution Function (CDF). Focusing on

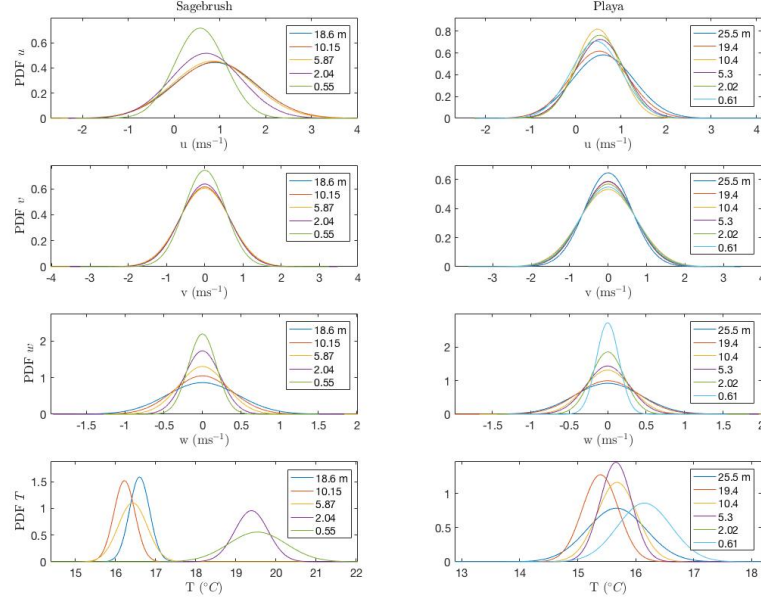


Figure 5: Collection of probability distributions from the Sagebrush (**left**) and the Playa (**right** sites). From top to bottom PDF  $u$ , PDF  $v$ , PDF  $w$  and PDF  $T$ .

Sagebrush					
$z$ (m)	Statistic	$u$	$v$	$w$	$T$
18.6	Kurtosis	2.3731	3.1820	3.6346	1.6588
	Skewness	0.3067	0.2446	0.8532	-0.3490
10.15	Kurtosis	2.4933	3.4515	2.8027	1.8469
	Skewness	0.1651	0.1227	0.3879	-0.5126
5.87	Kurtosis	2.6679	3.2820	3.8053	2.0491
	Skewness	0.2694	0.1717	0.5359	-0.6396
2.04	Kurtosis	2.6868	3.6466	3.3045	2.0662
	Skewness	0.1876	0.3174	0.4101	-0.4458
0.55	Kurtosis	2.6739	3.1869	3.8168	2.4663
	Skewness	0.0655	0.3693	0.3859	0.7037

Table 1: Skewness and kurtosis values for the Sagebrush site on October 19th from 1500-1530 MST.

Playa					
z (m)	Statistic	u	v	w	T
25.5	Kurtosis	2.1075	2.5910	3.5269	2.2656
	Skewness	0.1212	-0.2004	0.7672	0.5295
19.4	Kurtosis	2.2519	2.8332	3.4123	1.6080
	Skewness	0.2287	-0.2862	0.7324	0.1421
10.4	Kurtosis	2.8320	1.9469	3.0079	4.6
	Skewness	0.3884	0.1464	0.3786	1.2276
5.3	Kurtosis	2.9033	2.1528	3.1285	3.2123
	Skewness	0.1862	0.1298	0.4560	0.9190
2.02	Kurtosis	3.0038	2.0993	3.2620	2.3460
	Skewness	0.3980	-0.0969	0.4160	0.6531
0.61	Kurtosis	3.1414	1.9599	3.3634	2.3473
	Skewness	0.5253	-0.1403	0.2770	0.6531

Table 2: Skewness and kurtosis values for the Playa site on October 19th from 1500-1530 MST.

the third row (CDF  $w$ ) one can now see of the increased distribution of vertical velocities with height at both sites. This is due to the convective nature of the period of interest. Figure 7 presents the autocorrelation function for the velocity components and the temperature at both sites. The autocorrelation was computed for the 30 minutes of interest, 15 minutes is presented.  $u$ ,  $v$ , and  $T$  show fairly linearly decays with time, while  $w$  decays rapidly to 0. Interesting features in Figure 7 are seen in the autocorrelation of  $u$  at the Sagebrush and Playa. At the Sagebrush we observe a more rapid decay of correlation at the lower heights, while at the Playa, all heights share the same correlation with time (decreasing at similar rates). Additionally, further turbulence analysis was performed on the data from the two sites. Figure 8 presents the temperature with height (right) of the two sites, while the left column presents (from top to bottom) the mean velocity with height, instantaneous plots of  $u'$ ,  $v'$ , and  $w'$  with height. The data presented is only of the period of interest. From the temperature profile, we observe a large energy storage ( $2^{\circ}\text{C}$ ) at the surface layer compared to the Playa. In the mean velocity profile the impact of the sagebrush on the mean flow, creating a large drag at the surface, is clearly observed. Examination of the fluctuations reveals the fluctuations in the mean wind direction are larger in magnitude at the Playa with less variance compared to the Sagebrush, while the converse is observed for the cross wind component. The vertical fluctuations at both sites appear to increase in variance and magnitude with height. Figure 9 and Figure 10 presents the fluctuation correlations between the velocity components and their respective kinematic heat fluxes (Figure 9 at 0.5 m and Figure 10 at 20 m). At both heights for the velocity correlations the Sagebrush appears to contain larger fluctuations in each variable (larger spread). Suggesting an increase in TKE at this site. As expected at 0.5 m the heat flux correlations have very small velocity fluctuations, however larger temperature fluctuations exist,

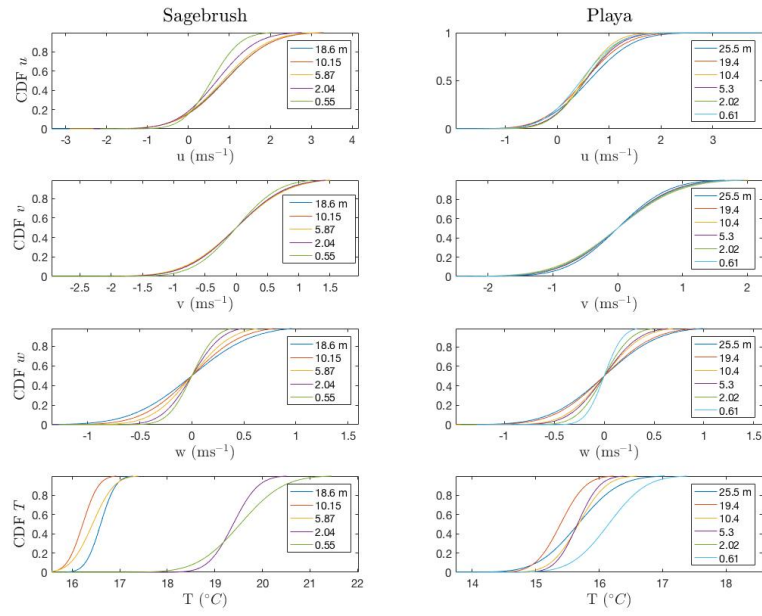


Figure 6: Collection of cumulative distributions from the Sagebrush (**left**) and the Playa (**right** sites). From top to bottom CDF  $u$ , CDF  $v$ , CDF  $w$  and CDF  $T$ .

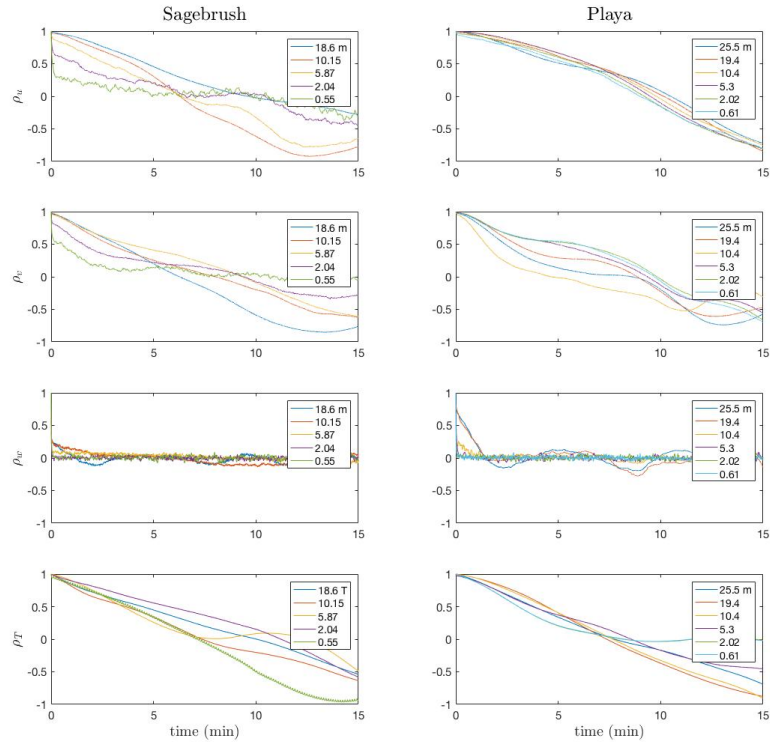


Figure 7: Collection of autocorrelations from the Sagebrush (**left**) and the Playa (**right** sites). From top to bottom  $\rho u$ ,  $\rho v$ ,  $\rho w$  and  $\rho T$  .



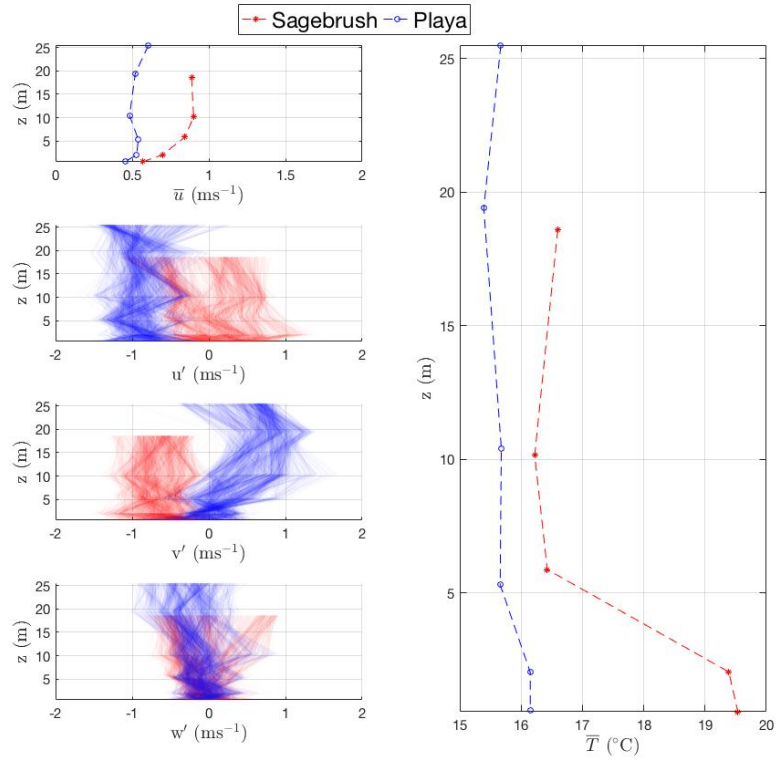


Figure 8: Sagebrush (red) and Playa (blue) mean velocity (top left), instantaneous velocity fluctuations at 20 Hz (left) and temperature (right) for each height during period of interest, 1500-1530 MST on October 19th, 2012

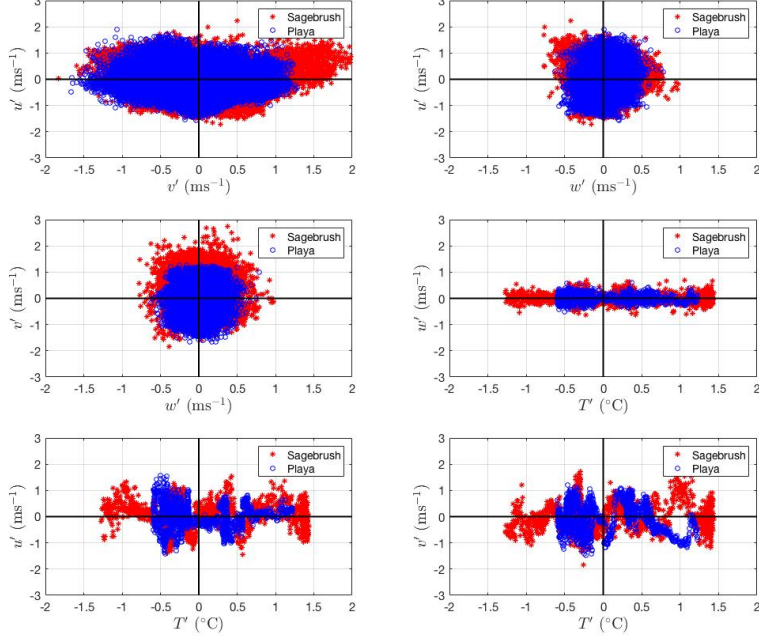


Figure 9: Correlations for momentum and heat flux for 0.5 m during period of interest, 1500-1530 MST on October 19th, 2012

suggesting the surface heterogeneity influencing the flow. Larger temperature fluctuations are seen at the Sagebrush then the Playa at the 0.5 m, suggesting the impact of temperature heterogeneity is affecting the flow more so at the Sagebrush site than the Playa site. Examination of the 20 m heat flux correlation suggests that the temperature fluctuations at both site match fairly well in magnitude, thus concluding the effect observed at the lower height from the Sagebrush, has been washed out by 20 m.

### 3 Conclusion

In an effort the better understand the impact of the surface roughness heterogeneities between the Playa and Sagebrush sites the authors have confined their findings to the following key results.

- The Sagebrush site has increased dissipation, energy storage, and larger contribution of high frequency eddies as a result of the increased surface roughness.
- The Playa site demonstrated stronger autocorrelations along all heights.

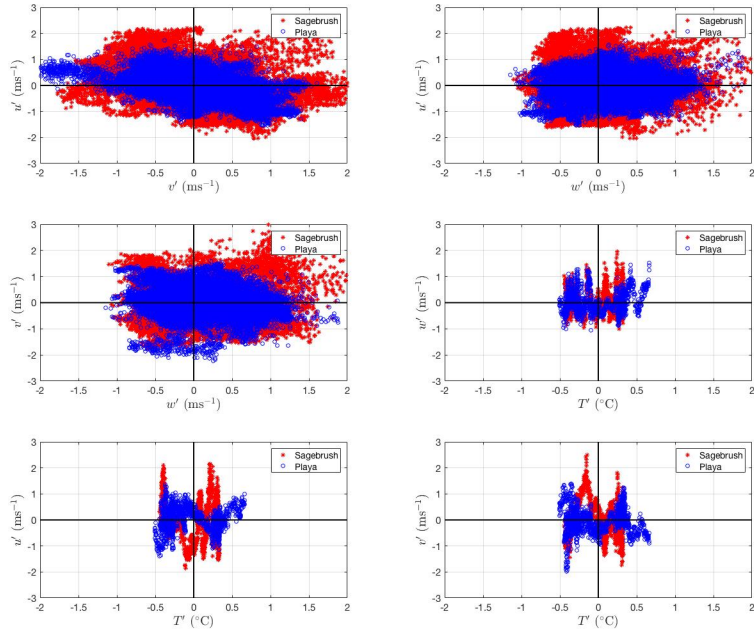


Figure 10: Correlations for momentum and heat flux for 20 m during period of interest, 1500-1530 MST on October 19th, 2012

- The impacts of the vegetation at the Sagebrush site diminish by 10 m.

Additionally the authors would like to examine the impact of different de-trending times, such as whose analysis utilizes a 5 minute de-trending period for evening transitions. Furthermore a more in depth analysis utilizing Multi-Resolution Decomposition during the time period to derive a time and length scale associated with the surface roughness heterogeneity.